INSTITUTE OF PHYSICS PUBLISHING WAVES IN RANDOM MEDIA

Waves Random Media **12** (2002) 365–385 PII: S0959-7174(02)33163-X

Focusing of time-reversed reflections

Knut Sølna

Department of Mathematics, University of California at Irvine, Irvine, CA 92697, USA

E-mail: ksolna@math.uci.edu

Received 28 January 2002
Published 16 May 2002
Online at stacks.iop.org/WRM/12/365

Abstract

Recently time-reversal techniques have emerged as a new, important and fascinating discipline within wave propagation. Many of the problems involved can best be understood, analysed and optimized based on a random field model for the medium. Here we discuss stable refocusing of second-order time-reversed reflections. This phenomenon may appear as surprising at first. However, we show how it can be understood in very simple terms viewing the wavefield as a stochastic process. We give sufficient conditions on Green's function of the propagation problem for the phenomenon to happen. In particular we discuss acoustic wave propagation in the regime of weak random medium fluctuations and explicitly give the derivation of stable refocusing in this case, illustrating it with numerical examples.

(Some figures in this article are in colour only in the electronic version)

1. Introduction

Recently techniques based on time reversal of wavefields have received a lot of attention [8, 9]. With time reversal we mean that the wave is recorded in time, like an acoustic signal on a tape recorder, then re-emitted time-reversed, like playing the tape in reverse. Surprising and fascinating physical effects can be synthesized in this way. Moreover, existing methods in, for instance, communication, imaging and for solving inverse problems can be improved in a fundamental way. The possibility of refocusing and super-resolution by time reversal has applications in medicine, geophysics, non-destructive testing, underwater acoustics, wireless communications, etc [3, 9, 10, 13].

In one kind of time-reversal experiment, a wavefield is recorded by an array of transducers, time-reversed, and then re-transmitted into the medium. The re-transmitted signal propagates back through the same medium and refocuses approximately at the original (localized) source point for the wavefield. Time reversal and back-propagation thus acts as an approximate inverse for the forward propagator of the wavefield. The refocusing is approximate because of the finite size of the array of transducers (receivers and transmitters), the *time-reversal mirror*.

In a homogeneous medium the re-focusing resolution of the time-reversed signal is limited by the size of the time-reversal mirror and of the length to the mirror, the diffraction limit. When the medium has random inhomogeneities the resolution of the refocused signal can, in some circumstances, *beat* the diffraction limit, which is called super-resolution [4, 7].

In the above time-reversal experiments the sharpening of the refocal spot caused by random fluctuations in the medium parameters is essentially a decoherence phenomenon. Only wave energy sharply focused toward the source will be coherent enough to make up a strong stable time-domain signal. In a second kind of time-reversal experiment the mechanism for generation of a sharply focused pulse after time reversal can rather be understood as a statistical coherence phenomenon. In this type of application there is *no* refocused pulse in the homogeneous case. Yet, in a randomly heterogeneous environment a refocused pulse emerges at the original (localized) source point. Moreover, despite the fact that the refocusing now is a purely statistical phenomenon, the shape of the refocused pulse is *non-random*. Below we shall refer to this phenomenon as *stabilization*. It is this second application of time reversal that we will analyse in detail in this paper. In this case the time-reversal mirror is located at the original source point and the received and time-reversed signal is sent back into the medium again rather than back toward the source.

The two time-reversal scenarios outlined above share one condition for sharp stable refocusing to occur: the presence of a separation of scales situation. It corresponds to the wavefield fluctuating on a scale that is fine relative to the size of the time-reversal mirror. In the next section we start the discussion of the second problem outlined above and explain this in more detail. We discuss how refocusing can be understood as a matching or coherence phenomenon and also illustrate it with some numerical experiments. In sections 3 and 4 we analyse the refocusing phenomenon. Here we take Green's function of the random medium as our starting point and give the conditions that will lead to stable refocusing. In sections 5 and 6 we consider the particular case with acoustic waves. We analyse this in detail in the regime of weak medium fluctuations and identify scaling scenarios that give a wavefield Green's function or propagator that results in stable refocusing. The results are illustrated with numerical computations.

2. Illustration of focusing

2.1. Numerical example

In this section we present a numerical illustration of the refocusing of time-reversed reflections in the case of acoustic waves propagating in one spatial dimension. The numerical simulations are based on an equal travel time discretization of the medium, as in [15]. The acoustic medium is randomly heterogeneous in the halfspace $x > 0$ with small zero mean fluctuations in the wave speed.

The numerical experiment is conducted as follows. First, we let a narrow wave pulse impinge upon the random medium. The wave reflected from the medium toward the source point will be small and incoherent since medium fluctuations are small and random. We next capture the signal in a time window centred at time t_0, reverse it in time and send it back into the medium. For one-dimensional acoustic wave propagation this corresponds exactly to

(i) capturing a spatial segment of the reflected signal travelling to the left at a particular time instant;
(ii) 'freezing' this piece and sending it back into the heterogeneous medium as a secondary right propagating source wave.

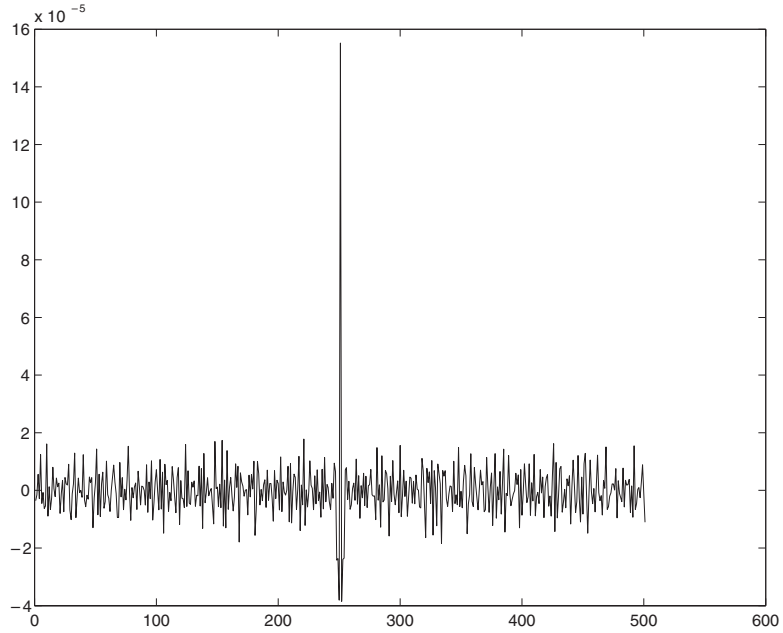

Figure 1. This figure shows the refocusing at the original source point for the second-order reflections from the random medium.

The second-order reflection generated by this *new* source is shown in figure 1, a time t_0 after we sent the signal into the heterogeneous medium. Note the focusing at the original source point for these second-order reflections. This is what we referred to as *refocusing* above. The refocusing is no coincidence. If we repeat the experiment with a *different* realization of the random medium we will see essentially the same refocused pulse. This is what we referred to as *stable* refocusing above. We next aim to describe qualitatively why this happens.

2.2. Response matching via time-reversal

To explain and quantify the focusing seen above we repeat the steps and illustrate it with some schematic cartoons.

The medium is heterogeneous in a halfspace, the halfspace $x > 0$, and homogeneous in the other half, as before. First we use an impulsive source located at the origin at time zero and impinging upon the random medium, see figure 2 (top). The bottom plot shows the first-order reflections from the random medium at time t_0 (call them $G(x)$). Since we used an impulsive source, the process $G(x)$ can be interpreted as the impulse response function of the medium or its random Green's function. We refer to the scale at which G fluctuates as l. Thus, we assume that $G(x)$ and $G(x + \Delta x)$ are approximately independent if $l \ll |\Delta x|$ and strongly correlated if $|\Delta x| \ll l$.

We again consider acoustic wave propagation and, just as above, cutting out a time piece, reversing this in time and sending it back into the medium corresponds to cutting out a spatial segment of the reflected wave, freezing it and sending it back into the medium by reversing its propagation direction. Thus, the trailing edge of the piece becomes the front when we re-emit it. The new source is shown as a full line in the top plot of figure 3. The second-order reflection is the convolution of the impulse response of the medium with this new source. However, the

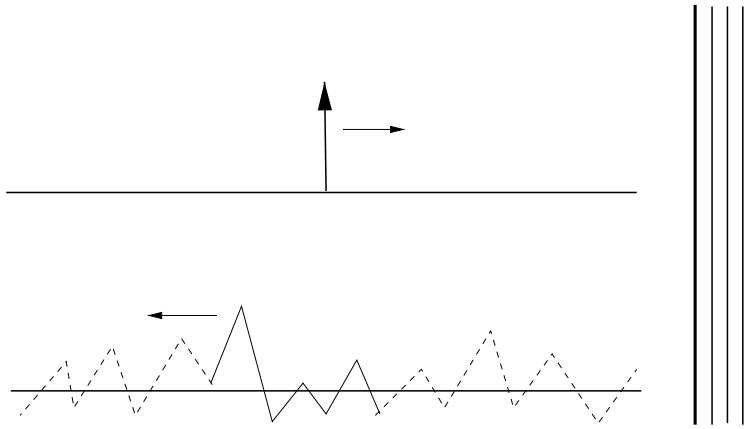

Figure 2. This figure illustrates the first-order reflections from an impulsive source. The top display shows the impinging impulse travelling to the right in the homogeneous halfspace and impinging upon the random or heterogeneous right halfspace. The bottom display shows the reflections, random Green's function or impulse response of the medium, evaluated a time t_0 later. The part of it that is shown with a full line is the part that corresponds to the window of width W, the segment that we capture, time-reverse and send back into the medium.

source was just a piece of the impulse response or Green's function itself. Due to the fact that we time reversed before re-emitting the signal, the convolution corresponds to sliding a piece of Green's function along itself and forming a local 'inner product', as illustrated in the middle display of figure 3. Evaluating the second-order reflection at time t_0 at the spatial origin corresponds to Green's function and the piece being exactly coherent before we form the inner product. Evaluating the reflection at time t_0, but a distance more than l from the origin corresponds to complete decoherence and a small inner product, thus giving re-focusing (as in figure 3 (bottom plot)) of a pulse that is moving to the left. The support of the refocused pulse will be $\mathcal{O}(l)$. To quantify the relative magnitude of the refocused pulse, assume that $X_n = G(nl)$ are zero mean, independently and identically distributed random variables. Let also $N = W/l$ with W the width of the window. The magnitude of the fluctuations relative to the refocused pulse is then of the order of

$$\frac{\sqrt{\mathrm{Var}[\sum_{i=1}^{N} X_i X_{i+\Delta}]}}{\mathbb{E}[\sum_{i=1}^{N} X_i^2]} = \mathcal{O}(N^{-1/2}).$$

Thus, the focusing phenomenon in time reversal is due to the matching of two copies of the response function of the (time-invariant) medium. It will occur when we have a *separation of scales*, in that the window width is large relative to the scale at which the response function decorrelates. The more detailed analysis carried out below confirms this picture.

3. Waves over a layered medium

3.1. Green's function

We analyse the focusing phenomenon in a one-dimensional medium. The random heterogeneous medium is located in the halfspace $z > z_0$. In the homogeneous halfspace we assume that the wave, u, can be decomposed as

$$u(t, z) = u_l(t + z/c_0) + u_r(t - z/c_0) \qquad \text{for } z \leqslant z_0, \tag{1}$$

with c_0 being the wave speed.

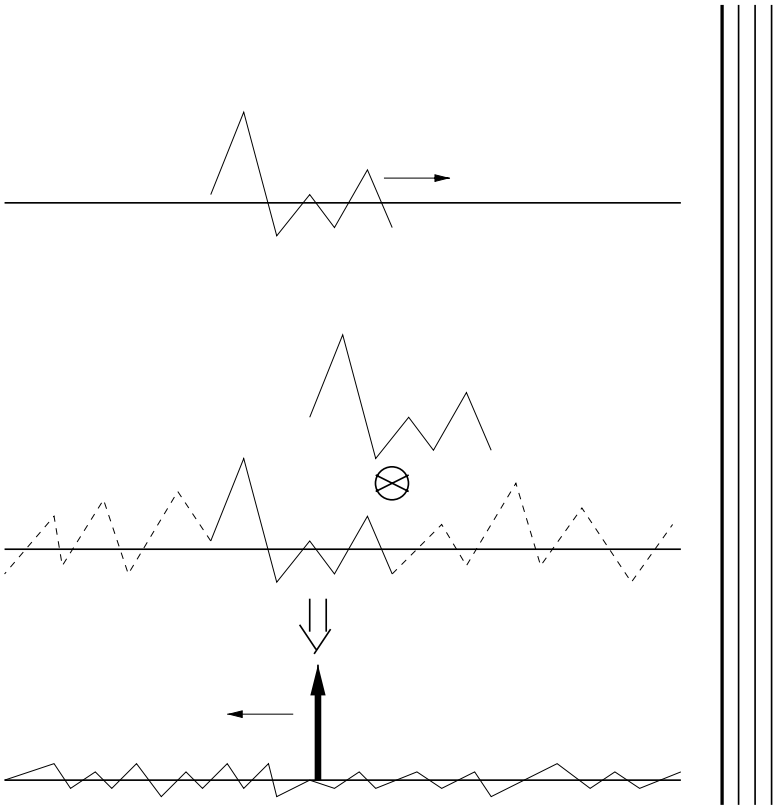

Figure 3. This figure illustrates the refocusing of the pulse. In the top display we show the source, the part of the reflected signal shown with a full line in figure 2. The direction of propagation has been changed and this piece is now impinging upon the random halfspace. The reflected signal will now be determined by sliding this piece of Green's function along itself and forming a local inner product. This gives the refocusing seen in the bottom plot.

We start by making a transformation to travel time depth coordinate to simplify notation: $x = z/c$, where c is the local speed. Then

$$u(t, x) = u_l(t + x) + u_r(t - x) \qquad \text{for } x \leqslant x_0. \tag{2}$$

Let the source or impinging waveshape be denoted by f. We assume a linear time-invariant medium and that for $u_r(t) = f(t)$:

$$u_l(t + x) = \int_{-\infty}^{\infty} G(t + x - s) f(s)\, \mathrm{d}s. \tag{3}$$

Thus, we model the heterogeneous medium in terms of the properties of a surface Green's function G that relates the impinging and reflected waves as stated in (1) and (3). In the next section we describe the time-reversal experiment and in section 3.3 we give the specific assumptions that we make about Green's function which lead to refocusing.

3.2. The time-reversal experiment

Denote the reflected wave process centred at time $t_0 > 0$ for r:

$$r(\tau, x) \equiv u_l(t_0 + \tau + x) = \int_{-\infty}^{\infty} G(t_0 + \tau + x - s) f(s)\, \mathrm{d}s.$$

As described in section 2.1 we first use an impulsive source travelling in the positive x direction with the medium being otherwise at rest. Second, we cut out a piece of the reflected signal and use this piece 'time reversed' as our new source. The reflected wave for the impulsive source, $f_1(t) = \delta(t)$, is

$$r_1(\tau, x) = G(t_0 + \tau + x).$$

The second source pulse, $f_2(t)$, is

$$f_2(t) = \begin{cases} r_1(-t, 0) & \text{for } |t| < W/2 \\ 0 & \text{else,} \end{cases} \tag{4}$$

which corresponds to applying a uniform window function centred at t_0 and width W. The reflected wave associated with the secondary source f_2 is

$$r_2(\tau, x) = \int_{-\infty}^{\infty} G(t_0 + \tau + x - s) f_2(s)\, \mathrm{d}s = \int_{-W/2}^{W/2} G(t_0 + \tau + x + s) G(t_0 + s)\, \mathrm{d}s, \tag{5}$$

which is the expression for the reflection process that is illustrated in figure 3.

3.3. Assumptions about Green's function

We want to characterize the reflected process and compute first its mean and variance:

$$\mathbb{E}[r_2(\sigma, 0)] = \int_{-W/2}^{W/2} \mathcal{R}(s; \sigma)\, \mathrm{d}s$$

$$\mathcal{R}(s; \sigma) \equiv \mathbb{E}[G(t_0 + s + \sigma) G(t_0 + s)] \tag{6}$$

$$\mathrm{Var}[r_2(\sigma, 0)] = \int_{-W/2}^{W/2} \int_{-W/2}^{W/2} \mathcal{R}_2(s, v; \sigma)\, \mathrm{d}s\, \mathrm{d}v$$

$$\mathcal{R}_2(s, v; \sigma) \equiv \mathbb{E}[X(s; \sigma) X(v; \sigma)]$$

$$X(s; \sigma) \equiv G(t_0 + s + \sigma) G(t_0 + s) - \mathcal{R}(s; \sigma). \tag{7}$$

Note that the reflected process is symmetric in space and time: $r_2(\sigma, 0) = r_2(0, \sigma)$.

Next, we make some assumptions about Green's function, G, that characterizes the reflected wavefield. We assume that G has mean zero and decorrelates for large offsets in its argument (assumptions (A_1) and (A_2) below). Thus, the medium does not generate any strong coherent reflections and the first-order reflections, r_1, are zero in the mean. Due to rapid decorrelation the second-order reflections, r_2, will refocus to a coherent pulse as in figure 3. The parameter l describes the scale at which Green's function decorrelates. Assumption (A_3) ensures that the reflections do not 'die out' within the window of width W and (A_4) that the centred process $X(s; \sigma)$ has a finite correlation length. The last two assumptions entail that the random fluctuations in the refocused pulse are relatively small for l small:

$$(A_1) \qquad \mathbb{E}[G] = 0$$

$$(A_2) \qquad \lim_{\sigma \to \infty} \sup_s |\mathcal{R}(s; \sigma)| = 0$$

$$(A_3) \qquad 0 < C_1 < \mathcal{R}(s, 0) \qquad \text{for } |s| < W/2$$

$$(A_4) \qquad \sup_{s,\sigma} \int_{-\infty}^{\infty} |\mathcal{R}_2(s, v; \sigma)|\, \mathrm{d}v = l < \infty.$$

Before we proceed, note that the above moments are not well defined for a singular Green's function associated with a medium generating strong reflections: however, this case can be considered using slightly smoothed initial data as in section 3.7.

3.4. Focusing in the mean

The above modelling trivially gives that the second-order reflection, r_2, focuses (in the mean):

Result 1. *The assumptions* $(A_{1,\dots,3})$ *imply that* $\forall \delta > 0 \, \exists \, M > 0$ *such that*

$$\frac{\mathbb{E}[r_2(\sigma, 0)]}{\mathbb{E}[r_2(0, 0)]} < \delta \qquad \text{for } \sigma > M.$$

Note that the focusing is symmetric in the space and time dimensions.

3.5. Separation of scales and stabilization

The modelling moreover easily gives that the random fluctuations in the reflection process are small relative to the magnitude of the focused pulse for large relative window width. This is what we refer to as *stabilization*:

Result 2. *The assumptions* $(A_{1,\dots,4})$ *imply that*

$$\frac{\sqrt{\mathrm{Var}[r_2(\sigma, 0)]}}{\mathbb{E}[r_2(0, 0)]} \leqslant \frac{1}{C_1\sqrt{N}}$$

with $N \equiv W/l$.

In the special case that $G(t)$ and $G(t + \tau)$ are independent for $|\tau| > l$, then (A_2) and (A_4) are satisfied for $\mathcal{R}_2$ bounded. If, moreover, $l \ll W$ the separation of timescales that we discussed in the introduction is present and we get stable refocusing.

3.6. Local stationarity

In this section we introduce some additional assumptions to get a more precise characterization of the focused reflections. We consider the case when the random fluctuations in r_2 are rapid relative to the window width, but when the *statistics* of the reflection process vary slowly relative to this scale. Thus, the window width *separates* the micro- and the macroscale in the reflection process. We make here the idealized stationarity assumption: the process $G(t_0+s+\sigma)G(t_0+s)$ is nearly stationary in s when observed for $|s| < W$. Then we find

$$\mathbb{E}[r_2(\sigma, 0)] = \int_{-W/2}^{W/2} \mathcal{R}(s, \sigma)\, \mathrm{d}s \approx W\mathcal{R}(0, \sigma) \tag{8}$$

and approximately:

$$\frac{\sqrt{\mathrm{Var}[r_2(\sigma, 0)]}}{\mathbb{E}[r_2(0, 0)]} < \sqrt{\frac{\int_{-\infty}^{\infty} |\mathcal{R}_2(0, v; \sigma)|/(\mathcal{R}(0, 0))^2 \, \mathrm{d}v}{W}}.$$

Thus, the shape of the refocused pulse is $\mathcal{R}(0, \sigma)$, the covariance function of Green's function evaluated relative to the centre of the time window. The relative magnitude of the fluctuations in the refocused pulse is bounded in terms of the correlation length of the process X relative to the window width.

3.7. General source and window functions

Consider now the more general case with a smooth source function, $f_1(t) = f(t)$, supported on an interval $\mathcal{O}(d)$ with $d \ll W$ and normalized such that $||f||_1 = 1$. Moreover, we introduce a window function $\mathcal{W}(t)$, supported for $|t| < W/2$, so that the secondary source as in (4) is

$$f_2(t) = \begin{cases} r_1(-t, 0)\mathcal{W}(-t) & \text{for } t < W/2 \\ 0 & \text{else.} \end{cases}$$

In this case

$$r_2(\tau, x) = \int_{-\infty}^{\infty} G(t_0 + \tau + x + s)\mathcal{W}(s) \int_{-\infty}^{\infty} G(t_0 + s - v) f(v)\, \mathrm{d}v\, \mathrm{d}s$$

and

$$\mathbb{E}[r_2(\sigma, 0)] = \int_{-\infty}^{\infty}\int_{-\infty}^{\infty} \mathcal{W}(s + v)\mathcal{R}(s, \sigma + v) f(v)\, \mathrm{d}v\, \mathrm{d}s. \tag{9}$$

Under the stationarity assumptions of the previous section we find

$$\mathbb{E}[r_2(\sigma, 0)] \approx [\mathcal{R}(0, \cdot) \star f(-\cdot)](\sigma) \int_{-\infty}^{\infty} \mathcal{W}(s)\, \mathrm{d}s \tag{10}$$

with $\star$ representing convolution. If we then assume that Green's function is mixing on the scale l we find

$$\frac{\sqrt{\mathrm{Var}[r_2(\sigma, 0)]}}{\mathbb{E}[r_2(0, 0)]} = \mathcal{O}\left(\sqrt{\frac{\max(l, d)}{W}}\right).$$

Thus, the reflections focus at the origin for time t_0. If $l \ll d$, then the support of the focused pulse is approximately that of the source pulse and the relative fluctuations of the order of $\mathcal{O}(\sqrt{d/W})$.

4. Three-dimensional effects

We summarize how the focusing generalizes to a two- or three-dimensional (time-invariant) medium. Analysis for a point source located over a layered medium is presented in [2]. An analysis of Green's function for a locally layered medium is presented in [14]. The heterogeneous random medium is located in the halfspace $z > z_0 > 0$. We assume that there is one lateral spatial dimension, denoted x; the three-dimensional case is analogous. The source is located at $(z, x) = (0, x_s)$ and we record the reflected field at the point of observation $(z, x) = (0, x_o)$. We again state the assumptions regarding the medium and the propagation phenomenon in terms of Green's function $G = G(t, x_s, x_o)$. As in the one-dimensional case we express the reflections observed at the surface $z = 0$ in terms of Green's function:

$$u(t, x_o, x_s) = \int_{-\infty}^{\infty} G(t - s, x_o, x_s) f(s)\, \mathrm{d}s, \tag{11}$$

with f being the source function.

We next describe the time-reversal experiment which is analogous to the experiment in the one-dimensional case. However, in this case we consider different source and receiver points. First, we use an impulsive source at the source point x_s. Next, we observe the reflections at x_o in a time segment around t_0 and use this segment, reversed in time, as a new source function with source location x_o. As we will show, a focused pulse will then emerge at x_s a time period t_0 after re-emission. Denote the reflections associated with the impulsive source r_1 by

$$r_1(\tau) = G(t_0 + \tau, x_o, x_s).$$

The secondary source located at x_o is

$$f_2(t) = \begin{cases} r_1(-t, 0) & \text{for } t < W/2 \\ 0 & \text{else.} \end{cases}$$

The reflections observed at a point in the vicinity of the original source point, $(z, x, t) = (0, x_s + \Delta x, t_0 + \tau)$, are

$$r_2(\tau, \Delta x) = \int_{-W/2}^{W/2} G(t_0 + s + \tau, x_s + \Delta x, x_o) G(t_0 + s, x_o, x_s)\, \mathrm{d}s.$$

Again we seek a characterization of the second-order reflections and compute the mean and variance for these:

$$\mathbb{E}[r_2(\tau, \Delta x)] = \int_{-W/2}^{W/2} \mathcal{R}(s; \tau, \Delta x)\, \mathrm{d}s$$

$$\mathcal{R}(s; \tau, \Delta x) \equiv \mathbb{E}[G(t_0 + s + \tau, x_s + \Delta x, x_o)G(t_0 + s, x_o, x_s)]$$

$$\mathrm{Var}[r_2(\tau, \Delta x)] = \int_{-W/2}^{W/2}\int_{-W/2}^{W/2} \mathcal{R}_2(s, v; \tau, \Delta x)\, \mathrm{d}s\, \mathrm{d}v$$

$$\mathcal{R}_2(s, v; \tau, \Delta x) = \mathbb{E}[X(s; \tau, \Delta x)X(v; \tau, \Delta x)]$$

$$X(s; \tau, \Delta x) = G(t_0 + s + \tau, x_s + \Delta x, x_o)G(t_0 + s, x_o, x_s) - \mathcal{R}(s; \tau, \Delta x).$$

We now make a set of assumptions about the statistical moments of Green's function. Assumption (B_1) below entails that the medium does not generate any strong coherent reflections. The essential aspect of the random field G that gives refocusing of the second-order reflections is that it decorrelates rapidly in space and time, assumption (B_2) below. As before, assumption (B_3) entails that the reflections do not 'die out' within the time window. The condition (B_4) ensures that the centred process $X(s; \tau, \Delta x)$ has a finite correlation length and gives stabilization in the case that the window width is large relative to this length l:

$$(B_1) \qquad \mathbb{E}[G] = 0$$

$$(B_2) \qquad \lim_{\tau\to\infty} \sup_{s,\Delta x} |\mathcal{R}(s; \tau, \Delta x)| = 0$$

$$\lim_{\Delta x\to\infty} \sup_{s,\tau} |\mathcal{R}(s; \tau, \Delta x)| = 0$$

$$(B_3) \qquad 0 < C_2 < \mathcal{R}(s; 0, 0) \qquad \text{for } |s| < W$$

$$(B_4) \qquad \sup_{s,\tau,\Delta x} \int_{-\infty}^{\infty} |\mathcal{R}_2(s, v; \tau, \Delta x)|\, \mathrm{d}v = l < \infty.$$

These assumptions give refocusing:

Result 3. *The assumptions* $(B_{1,\ldots,3})$ *imply that* $\forall\delta > 0\, \exists\, M > 0$ *such that*

$$\frac{\mathbb{E}[r_2(\tau, \Delta x)]}{\mathbb{E}[r_2(0, 0)]} < \delta \qquad \textit{for } \min(|\tau|, |\Delta x|) > M.$$

Therefore, at the surface $z = 0$ the mean reflection focuses at the original source point for time $t = t_0$. The support in time, (τ), and space, (Δx), of the refocused pulse will be on the scale at which $\mathcal{R}$ decorrelates in these variables. The stabilization property seen in the one-dimensional case prevails:

Result 4. *The assumptions* $(B_{1,\ldots,4})$ *imply that*

$$\frac{\sqrt{\mathrm{Var}[r_2(\tau, \Delta x)]}}{\mathbb{E}[r_2(0, 0)]} \leqslant \frac{1}{C_2\sqrt{N}}$$

with $N \equiv W/l$.

Note that if Green's function satisfies the reciprocity property:

$$G(t, x_s, x_o) = G(t, x_o, x_s),$$

then

$$\mathcal{R}(s; \tau, \Delta x) = \mathbb{E}[G(t_0 + s + \tau, x_s + \Delta x, x_o)G(t_0 + s, x_s, x_o)]$$

and the above assumptions correspond to Green's function decorrelating rapidly in the source coordinates.

5. Acoustic waves

5.1. Refocusing in the acoustic case

In this section we consider the acoustic case with the random medium fluctuations modelled by stochastic processes. The governing equations are the conservation laws for momentum and mass:

$$\begin{aligned} &\rho(x)\frac{\partial}{\partial t}u(t,x)+\frac{\partial}{\partial x}p(t,x)=0,\\ &\frac{1}{K(x)}\frac{\partial}{\partial t}p(t,x)+\frac{\partial}{\partial x}u(t,x)=0 \end{aligned} \tag{12}$$

with $p(t,x)$ being pressure and $u(t,x)$ velocity. The material parameters ρ and K are, respectively, the density and bulk modulus. We let L denote the macroscale in our problem. This length scale corresponds to the propagation distance for the signal in between emission and recording times. The 'microscale' corresponds the characteristic spatial scale at which the medium fluctuates. We take this scale to be εL with ε a dimensionless small parameter. The medium model is

$$\begin{aligned} \rho(x) &= \begin{cases} \rho_0\Big[1+\sqrt{\varepsilon}\eta\Big(\dfrac{x}{\varepsilon L}\Big)\Big] & \text{for } x>0\\ \rho_0 & \text{else,} \end{cases}\\ \frac{1}{K(x)} &= \begin{cases} \dfrac{1}{K_0}\Big[1+\sqrt{\varepsilon}\nu\Big(\dfrac{x}{\varepsilon L}\Big)\Big] & \text{for } x>0\\ \dfrac{1}{K_0} & \text{else} \end{cases} \end{aligned} \tag{13}$$

where the random fluctuations $c_1 < \nu < c_2$ and $c_3 < \eta < c_4$ are mean zero stationary stochastic processes and the halfspace $x \leqslant 0$ is homogeneous. In section 6 we consider the more general case when the mean density $\rho_0 = \rho_0(x)$ and the mean bulk modulus $K_0 = K_0(x)$ are assumed to be differentiable functions of x. The above model is the one introduced and analysed in [5], the difference being the factor $\sqrt{\varepsilon}$ multiplying the random fluctuations. Thus, we consider here a *weakly* fluctuating medium whereas the analysis presented in [5] concerns a strongly fluctuating medium. The smooth, compactly supported in $[0,\infty)$ source wavelet is

$$f_1(t) = f\left(\frac{t}{\varepsilon}\right).$$

Observe that we let the source pulse be *supported on the microscale*. Hence there will be a strong interaction between the pulse and the microscale medium variations. The small-scale noise in the medium model gives a non-coherent backscattering. As discussed above, these we capture in a time window and use as a secondary source wavelet, after time reversal. In the homogeneous halfspace we can decompose the wavefield as

$$\begin{aligned} u &= [f_1(t-x/c_0)+g(t+x/c_0)]/\zeta_0\\ p &= f_1(t-x/c_0)+g(t+x/c_0), \end{aligned}$$

with $\zeta_0 = \sqrt{K_0\rho_0}$ being the acoustic impedance and $c_0 = \zeta_0/\rho_0$ the acoustic sound velocity in this halfspace. Thus, the initial boundary condition that gives the primary source, a left-travelling wave pulse that strikes $x = 0$ at time $t = 0$, is

$$\begin{aligned} u &= \frac{f_1(t-x/c_0)}{\zeta_0}\\ p &= f_1(t-x/c_0) \end{aligned}$$

for $t \leqslant t_m$. We write the first-order reflections generated by this source as

$$r_1(\tau) = p(t_0 + \tau, 0) = [G \star f_1](t_0 + \tau),$$

with G being the surface Green's function. We capture these reflections in a window and then reverse time to get the secondary source:

$$f_2(-t) \equiv r_1(t)\mathcal{W}(t)$$

with $\mathcal{W}$ being a window function and defined as before. The initial boundary condition with the secondary source is

$$u_2 = \frac{f_2(t - x/c_0)}{\zeta_0}$$
$$p_2 = f_2(t - x/c_0),$$

for $t \leqslant t_m$. The corresponding secondary reflections become

$$r_2(\tau) = p_2(t_0 + \tau, 0) = [G \star f_2](t_0 + \tau) = [G(\cdot) \star [G \star f_1](t_0 - \cdot)\mathcal{W}(-\cdot)](t_0 + \tau).$$

This wavefield refocuses stably for small τ. We show in section 6:

Result 5. *Assume that $\eta(s)$ and $\nu(s)$ are bounded, stationary ergodic Markov processes, then in probability*

$$\lim_{\varepsilon \to 0} r_2(\varepsilon\sigma) = \int_{-\infty}^{\infty}\int_{-\infty}^{\infty} \bar{\mathcal{R}}(s, \sigma + v)\mathcal{W}(s) f(v)\, \mathrm{d}v\, \mathrm{d}s$$

as in (9) and (22). The function $\bar{\mathcal{R}}$ can formally be interpreted as the covariance of Green's function:

$$\bar{\mathcal{R}}(s, \sigma) = \lim_{\varepsilon \to 0} \mathbb{E}[G(t_0 + s + \varepsilon\sigma)G(t_0 + s)],$$

and is given by

$$\bar{\mathcal{R}}(s, \sigma) = \frac{1}{2\pi}\int \frac{\omega^2\hat{\alpha}(2\omega)}{(1 + \omega^2\hat{\alpha}(2\omega)^2(t_0 + s)/t_L)} \mathrm{e}^{-\mathrm{i}\omega\sigma/t_L}\, \mathrm{d}\omega \tag{14}$$

with $t_L = L/c_0$ and $\hat{\alpha}$ being the power spectral density of the medium fluctuations:

$$\hat{\alpha}(\omega) = \int_0^{\infty} \alpha(s)\cos(\omega s)\, \mathrm{d}s \equiv \int_0^{\infty} \mathbb{E}\left[\frac{\eta(s) + \nu(s)}{2}\right]\cos(\omega s)\, \mathrm{d}s.$$

Note that the surface Green's function therefore decorrelates on the scale ε.

Consider now the case with the medium model:

$$\rho(x) = \begin{cases} \rho_0 l\left[1 + \sqrt{\varepsilon\delta}\eta\left(\dfrac{x}{\varepsilon L}\right)\right] & \text{for } x > 0 \\ \rho_0 & \text{else} \end{cases}$$

$$\frac{1}{K(x)} = \begin{cases} \dfrac{1}{K_0}\left[1 + \sqrt{\varepsilon\delta}\nu\left(\dfrac{x}{\varepsilon L}\right)\right] & \text{for } x > 0 \\ \dfrac{1}{K_0} & \text{else,} \end{cases}$$

with $\varepsilon \ll \delta \leqslant \mathcal{O}(1)$. Thus, the medium fluctuations are weaker than in the case we considered above. The above result prevails in this case when $t_0 \mapsto t_0/\delta$ and $\mathcal{W}(\cdot) \mapsto \mathcal{W}(\delta\cdot)$. Thus, for a homogeneous medium the shape of the refocused pulse is essentially not affected by δ if t_0 is replaced by t_0/δ such that the wave penetrates deeper into the medium to compensate for the weaker fluctuations.

Consider finally the case with δ small and t_0 fixed. Then

$$\lim_{\varepsilon\to 0} r_2(\varepsilon\sigma) \propto [\alpha(\cdot/2) \star f''(\cdot)](-\sigma) \tag{15}$$

and in the low frequency case with f being smooth relative to the support of α:

$$\lim_{\varepsilon\to 0} r_2(\varepsilon\sigma) \propto f''(-\sigma).$$

5.2. Numerical illustration

The reflected acoustic field for a one-dimensional medium can be accurately calculated using a equal travel time discretization of the medium. We show numerically calculated refocused second-order reflections for the discretized approximation. The medium corresponds to the following random medium model for the local speed of sound:

$$c^2(x) = c_0^2\left(1 + \sigma\sqrt{\varepsilon}\nu\left(\frac{x}{\varepsilon}\right)\right),$$

where ν is a homogeneous Markov process with correlations

$$\mathbb{E}[\nu(x+\Delta)\nu(x)] = \mathrm{e}^{-\Delta x}.$$

This model gives

$$\bar{\mathcal{R}}(s,\sigma) = C(s)\left[\delta(\sigma) - \frac{\mathrm{e}^{-|\sigma|/\beta}}{2\beta}\{1 - \alpha/4(1 - |\sigma|/\beta)\}\right] \tag{16}$$

with

$$\alpha = t_0\sigma^2$$
$$\beta = 2\sqrt{1+\alpha/2}.$$

We use an impulsive source, $\varepsilon \approx 10^{-3}$, $W = 400\varepsilon$ and show the refocused second-order reflections for small, medium and large values of α.

Figure 4 corresponds to the medium fluctuations being small $\alpha \approx 0$. This figure indeed shows that the refocused pulse, corresponding to the autocorrelation for Green's function, essentially is, weakly, the second derivative. The broken curve is model (16) when we have normalized the pulses in magnitude.

In figure 5 we show the case with larger medium fluctuations and $\alpha = 10$. The figure shows that the refocused pulse is close to being the impulse in this case.

The next figure, figure 6, corresponds to a relatively narrow window $W = 100\varepsilon$ and to a large α: $\alpha = 70$. We show the refocused pulse for 20 realizations of the random medium. We clearly see the exponential structure in the refocused pulses, but the fluctuations around the mean shape are large. In figure 7 we show the refocused pulses with a broader window: $W = 400\varepsilon$, but with the same value for α. The fluctuations have been reduced by approximately a factor of a half, as they would according to result 2.

5.3. Result by Clouet and Fouque

For one-dimensional acoustic waves Clouet and Fouque give in [6] a nice derivation of the focusing phenomenon based on the expressions for the moments of the field obtained in [1]. They consider the scaling scenario where the medium fluctuations are strong $\mathcal{O}(1)$ and the source function smooth relative to the scale of the medium fluctuations. This corresponds to $l \ll d$ in the notation of section 3.7.

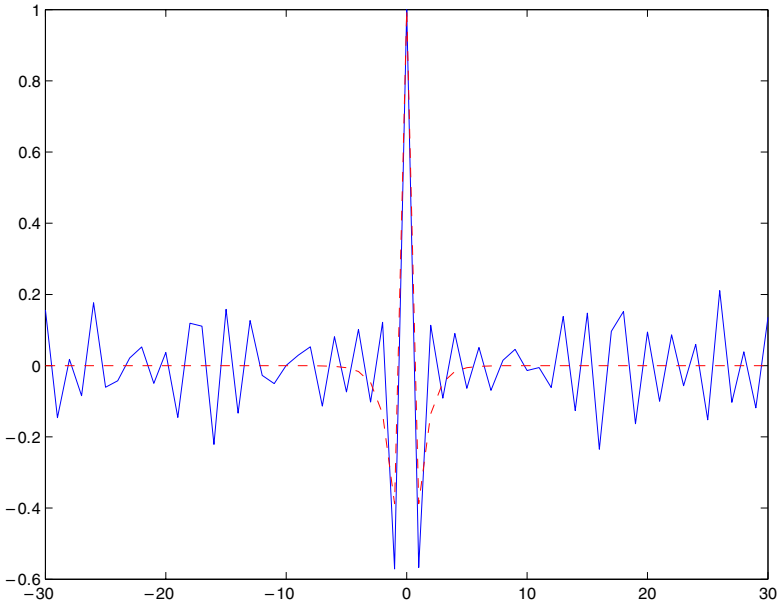

Figure 4. This figure shows the refocused pulse when the medium fluctuations are very small. Note that the pulse is a discrete version of the second derivative operator. The broken curve is model (16).

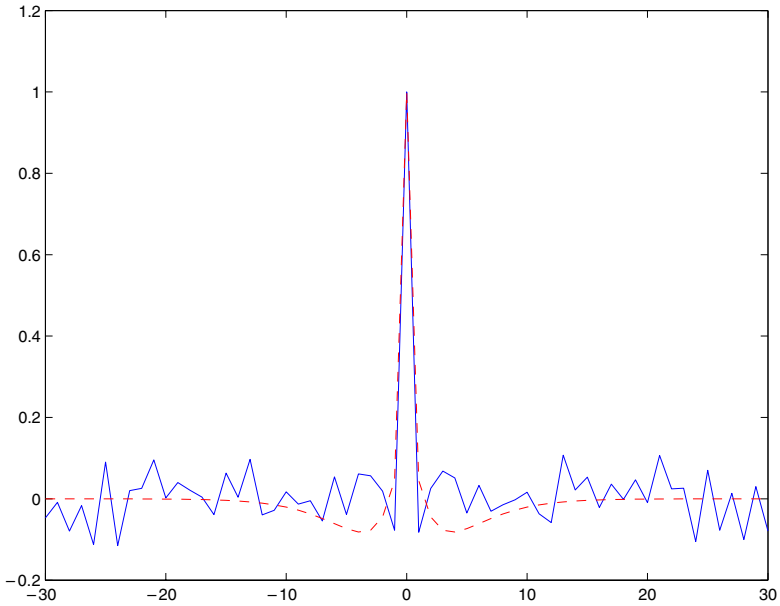

Figure 5. This figure shows the refocused pulse when the medium fluctuations are larger than in the previous figure. The pulse shape corresponds to an impulse. The broken curve is model (16).

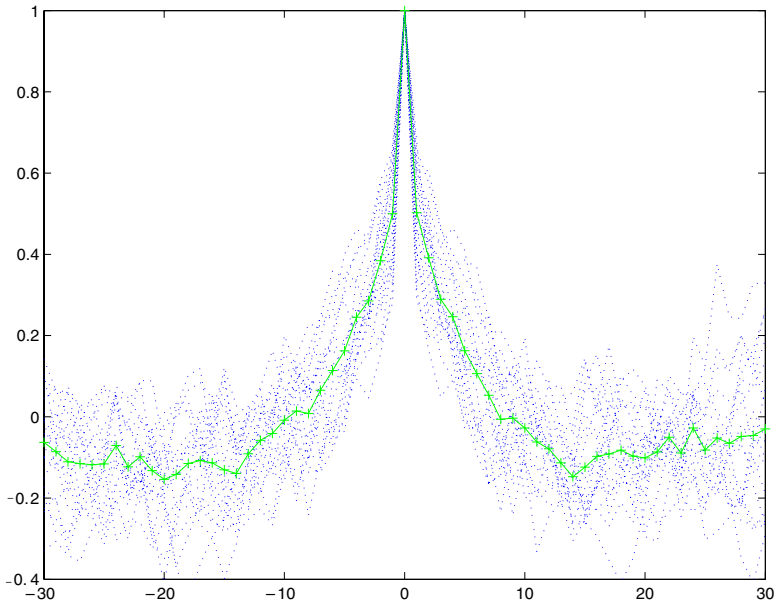

Figure 6. This figure displays refocused pulses for several independent realizations of the random medium. The window width, W, is small and the fluctuations in the pulse shapes large. The full curve is the average pulse shape.

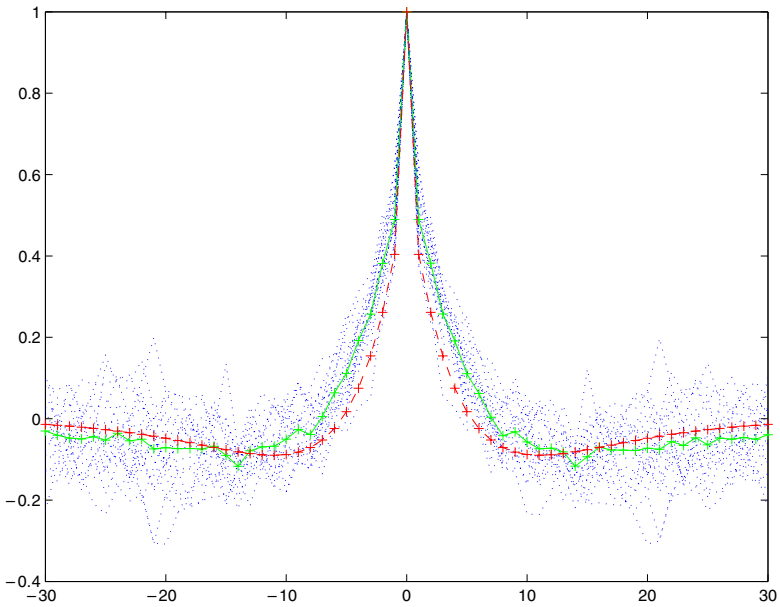

Figure 7. This figure displays refocused pulses for several independent realizations of the random medium. The window width, W, is larger than in the previous figure and the fluctuations in the pulse shapes smaller. Thus, the figure illustrates the stability in the pulse shape with respect to the particular medium realization for large window widths. The broken curve is model (16) and the full curve the average pulse shape.

In the previous section we considered the case with $l \approx d$ and hence a stronger interaction of the pulse with the statistics of the medium. We here connect their result to the above. Let the governing equations be (12) with model parameters

$$\rho(x) = \begin{cases} (\bar{K}/c_0^2)\left[1 + \eta\left(\dfrac{x}{\varepsilon}\right)\right] & \text{for } x > 0 \\ (\bar{K}/c_0^2) & \text{else,} \end{cases}$$
$$K(x) \equiv \bar{K}$$

and initial source function

$$f_1(t) = f\left(\frac{t}{\sqrt{\varepsilon}}\right).$$

It is shown in [6] that the second-order reflections can then be expressed as

$$\lim_{\varepsilon \to 0} \mathbb{E}[r_2(t_0 + \sqrt{\varepsilon}\sigma)] = \int_{-\infty}^{\infty} \mathrm{e}^{-\mathrm{i}\omega\sigma} \overline{\hat{f}}(\omega)[\Lambda(\omega, t) \star G(t)](t_0)\, \mathrm{d}\omega \tag{17}$$

with

$$\Lambda(\omega, t) = \frac{\omega^2 \hat{\alpha}(0)}{(1 + \omega^2 \hat{\alpha}(0) t_0)^2}. \tag{18}$$

This expression can be rewritten in the form (9) with $\mathcal{R}$ the transform of Λ and with the long wavelength limit of (14) matching the weak noise limit of (17).

5.4. Connection to localization

The form

$$\frac{\omega^2 \sigma^2}{(1 + \omega^2 \sigma^2 t_0)^2} \tag{19}$$

for the local power spectrum of Green's function corresponds to the above and entails that the refocused pulse is approximately

$$\sigma^2 f''$$

for t_0 small. Next, we give a heuristic motivation. With small t_0 mostly first-order scattering events close to the surface contribute to the reflected signal. Consider a discrete approximation of the medium. Then a large interface reflection coefficient of magnitude, say σ, is followed by a second of approximately opposite magnitude, $-\sigma$. With the probing pulse being smooth relative to the fluctuations this means that the backscattered signal scales like $\sigma f'$. The second-order time-reversed signal thus scales like $\sigma^2 f''$. A correction to this picture can be obtained by recalling that the frequency-dependent localization length in the above acoustic case is approximately

$$l_{loc} = \frac{c_0}{2\omega^2 \sigma^2}.$$

This suggests the following approximation for the 'transmission loss' for the first-order reflections from a shallow depth $L = c_0 t_0/2$:

$$\mathrm{e}^{-L/l_{loc}} \approx \frac{1}{1 + \omega^2 \sigma^2 t_0}.$$

A local 'reflexivity' $\sigma\omega$, together with this transmission loss, suggests the form (19) for the power spectrum.

6. Derivation for acoustic waves

6.1. Problem formulation

We summarize here the derivation of result 5 for the refocused pulse in the acoustic case with weak medium fluctuations. The method used is the one set forth in [5] adapted to the case with weak medium fluctuations and a probing pulse that is supported on the microscale rather than being smooth relative to this scale. We consider the model defined by (12) and let the parameters be defined by

$$\rho(x) = \begin{cases} \rho_0\Big(\dfrac{x}{L}\Big)\Big[1 + \sqrt{\varepsilon}\eta\Big(\dfrac{x}{\varepsilon L}\Big)\Big] & \text{for } x > 0 \\ \rho_0(0) & \text{else} \end{cases}$$
$$\frac{1}{K(x)} = \begin{cases} \dfrac{1}{K_0(x/L)}\Big[1 + \sqrt{\varepsilon}\nu\Big(\dfrac{x}{\varepsilon L}\Big)\Big] & \text{for } x > 0 \\ \dfrac{1}{K_0(0)} & \text{else.} \end{cases} \tag{20}$$

The mean density ρ_0 and the mean bulk modulus K_0 are assumed to be differentiable functions of x. Following [5] we non-dimensionalize by setting

$$x' = \frac{x}{L} \qquad p' = \frac{p}{\rho_0(0)c_0(0)^2}$$
$$t' = \frac{c_0(0)t}{L} \qquad u' = \frac{u}{c_0(0)}$$
$$\rho_0'(x') = \frac{\rho_0(x')}{\rho_0(0)} \qquad K_0'(x') = \frac{K_0(x')}{K_0(0)}.$$

After dropping primes we find in non-dimensionalized units

$$\rho(x)\frac{\partial}{\partial t}u(t,x) + \frac{\partial}{\partial x}p(t,x) = 0,$$
$$\frac{1}{K(x)}\frac{\partial}{\partial t}p(t,x) + \frac{\partial}{\partial x}u(t,x) = 0$$

with $\rho_0(x) \equiv 1$, $K_0(x) \equiv 1$ and $c_0(x) \equiv 1$ for $x \leqslant 0$. Next, we Fourier transform in time as

$$\hat{u}(\omega, x) = \int \mathrm{e}^{\mathrm{i}\omega t/\varepsilon} u(t,x)\,\mathrm{d}t$$
$$\hat{p}(\omega, x) = \int \mathrm{e}^{\mathrm{i}\omega t/\varepsilon} p(t,x)\,\mathrm{d}t$$

and introduce the 'travel time' from the origin according to the smooth background medium by

$$\tau(x) = \int_0^x \frac{\mathrm{d}s}{c_0(s)}.$$

We also decompose in left-going, A, and right-going, B, waves:

$$\hat{u} = \frac{1}{(K_0\rho_0)^{1/4}}[A\mathrm{e}^{-\mathrm{i}\omega\tau/\varepsilon} + B\mathrm{e}^{\mathrm{i}\omega\tau/\varepsilon}]$$
$$\hat{p} = (K_0\rho_0)^{1/4}[-A\mathrm{e}^{-\mathrm{i}\omega\tau/\varepsilon} + B\mathrm{e}^{\mathrm{i}\omega\tau/\varepsilon}]$$

with the decomposition being defined according to the smooth background medium. An incoming impulse at $x = 0$ corresponds to $B_1(\omega) = B(0;\omega) \equiv 1$ and then the transformed Green's function is $\hat{G}(\omega) = R(0;\omega) = A(0;\omega)$, where we introduced the reflection coefficient $R = A/B$. In section 6.3 we discuss further the equation and boundary conditions for R and obtain a characterization of Green's function G.

6.2. First- and second-order reflections

First, let the source wavelet be

$$f_1(t) = f(t/\varepsilon)$$

with Fourier transform

$$\hat{f}(\omega) = \int \mathrm{e}^{\mathrm{i}\omega t} f(t)\,\mathrm{d}t.$$

This is the probing right-going source when evaluated at the origin $x = 0$ and corresponds to $B_1(\omega) = \varepsilon \hat{f}(\omega)$. We choose a scaling such that the source wavelet is $\mathcal{O}(1)$ in magnitude, but this choice is not important as the problem is linear. The first-order reflection, the left-going wavelet, generated by the source and evaluated at $x = 0$ is

$$r_1(t) = \frac{1}{2\pi\varepsilon}\int \hat{G}(\omega)B_1(\omega)\mathrm{e}^{-\mathrm{i}\omega t/\varepsilon}\,\mathrm{d}\omega = \frac{1}{2\pi}\int \hat{G}(\omega)\hat{f}(\omega)\mathrm{e}^{-\mathrm{i}\omega t/\varepsilon}\,\mathrm{d}\omega.$$

We capture the reflections at time t_0 and apply the window function $\mathcal{W}$ before we time reverse to get the secondary source wavelet:

$$f_2(t) = r_1(t_0 - t)\mathcal{W}(-t),$$

which corresponds to

$$B_2(\omega) = \frac{1}{2\pi}\int \hat{G}(-(\omega+\varepsilon h))\,\hat{f}(-(\omega+\varepsilon h))\hat{\mathcal{W}}(h)\mathrm{e}^{\mathrm{i}t_0(h+\omega/\varepsilon)}\,\mathrm{d}h.$$

The reflections associated with this second right-going source wavelet is, when evaluated at $x = 0$,

$$\begin{aligned} r_2(t) &= \frac{1}{2\pi}\int \hat{G}(\omega)A_2(\omega)\mathrm{e}^{-\mathrm{i}\omega t/\varepsilon}\,\mathrm{d}\omega \\ &= \frac{1}{(2\pi)^2}\int \hat{G}(\omega-\varepsilon h)\hat{G}(-\omega)\,\hat{f}(-\omega)\hat{\mathcal{W}}(h)\mathrm{e}^{\mathrm{i}\omega(t_0-t)/\varepsilon}\mathrm{e}^{\mathrm{i}ht}\,\mathrm{d}\omega\,\mathrm{d}h, \end{aligned}$$

with $\hat{\mathcal{W}}$ being the unscaled Fourier transform of $\mathcal{W}$. We introduce next the spectrum

$$\Lambda(t,\omega) = \frac{1}{2\pi}\int \mathbb{E}[\hat{G}(\omega-\varepsilon h)\hat{G}(-\omega)]\mathrm{e}^{\mathrm{i}ht}\,\mathrm{d}h. \tag{21}$$

The mean reflected process can then be written as

$$\mathbb{E}[r_2(t)] = \frac{1}{2\pi}\int \Lambda(t-s,\omega)\mathcal{W}(-s)\,\mathrm{d}s\,\mathrm{e}^{\mathrm{i}\omega((t_0-t)/\varepsilon-\tau)}\,\mathrm{d}\omega\,f(\tau)\,\mathrm{d}\tau.$$

In the next section we shall obtain an explicit expression for the power spectrum Λ. We introduce also

$$\mathcal{R}_1(t,s) = \frac{1}{2\pi\varepsilon}\int \Lambda(t,\omega)\mathrm{e}^{-\mathrm{i}\omega s/\varepsilon}\,\mathrm{d}\omega.$$

The expression for the mean reflected pressure is then

$$\begin{aligned} \mathbb{E}[r_2(t)] &= \varepsilon\int \mathcal{R}_1(t-s,t-t_0+\varepsilon\tau)\mathcal{W}(-s)\,\mathrm{d}s\,f(\tau)\,\mathrm{d}\tau \\ &= \int \mathcal{R}_1(t-s,t-t_0+\tau)\mathcal{W}(-s)\,\mathrm{d}s\,f_1(\tau)\,\mathrm{d}\tau. \end{aligned}$$

It follows from the result of the next section that $\mathcal{R}_1$ has support $\mathcal{O}(\varepsilon)$ in its second argument which is the scale of the correlation length of the medium. Thus, only if $t - t_0 = \mathcal{O}(\varepsilon)$ will we see a refocused pulse. For $t = t_0 + \varepsilon\sigma$ we find

$$\mathbb{E}[r_2(t_0+\varepsilon\sigma)] = \int \mathcal{R}_1(t_0+\varepsilon\sigma-s,\varepsilon\sigma+\tau)\mathcal{W}(-s)\,\mathrm{d}s\,f\left(\frac{\tau}{\varepsilon}\right)\mathrm{d}\tau. \tag{22}$$

Thus, first the statistics of the 'locally stationary' covariance of Green's function is averaged with respect to the window function, then this mean covariance is averaged with respect to the source wavelet. The source wavelet is chosen to be supported on the scale at which Green's function decorrelates. Formally we have

$$\mathcal{R}_1(t_0+t,s)=\mathbb{E}[G(t_0+t)G(t_0+t-s)]=\mathcal{R}(t,-s)$$

with $\mathcal{R}$ defined as in (6). Hence

$$\mathbb{E}[r_2(t_0+\sigma)]=\int_{-\infty}^{\infty}\int_{-\infty}^{\infty}\mathcal{W}(s+v)\mathcal{R}(s,\sigma+v)\,f_1(v)\,\mathrm{d}v\,\mathrm{d}s,$$

which is (9).

6.3. The power spectrum

We summarize here how the expression for $\Lambda(t,\omega)$ introduced in (21) can be derived. This expression, corresponding to the autocorrelation of the surface Green's function, defines the (mean) shape of the refocused pulse. In the next subsection we discuss stabilization (i.e. the random fluctuations in the refocused pulse are small). The argument as presented here is formal. However, steps involving interchange of limits and choice of boundary conditions can be made rigorous using the method of functionals introduced in [5, 12].

We seek an expression for

$$\hat{\mathcal{R}}(\omega,h)\equiv\mathbb{E}[\hat{G}(\omega-\varepsilon h/2)\overline{\hat{G}}(\omega+\varepsilon h/2)].$$

Then

$$\Lambda(t,\omega)=\frac{1}{2\pi}\int\hat{\mathcal{R}}(\omega-\varepsilon h/2,h)\mathrm{e}^{\mathrm{i}ht}\,\mathrm{d}h\sim\frac{1}{2\pi}\int\hat{\mathcal{R}}(\omega,h)\mathrm{e}^{\mathrm{i}th}\,\mathrm{d}h\qquad\text{as }\varepsilon\downarrow 0.\tag{23}$$

Recall that $\hat{G}(\omega)=R(0;\omega)$, with $R=A/B$ being the reflection coefficient introduced above. From (12) and (20) it follows that the equations for the 'right/left-going' amplitudes are

$$\frac{\mathrm{d}}{\mathrm{d}x}\begin{bmatrix}A\\B\end{bmatrix}=\frac{\mathrm{i}\omega}{\sqrt{\varepsilon}}\left(\frac{\rho_0}{K_0}\right)^{1/2}\begin{bmatrix}-m & -n\mathrm{e}^{2\mathrm{i}\omega\tau/\varepsilon}\\ n\mathrm{e}^{-2\mathrm{i}\omega\tau/\varepsilon} & m\end{bmatrix}\begin{bmatrix}A\\B\end{bmatrix}$$
$$+\frac{1}{4}\frac{(K_0\rho_0)'}{(K_0\rho_0)}\begin{bmatrix}0 & \mathrm{e}^{2\mathrm{i}\omega\tau/\varepsilon}\\ \mathrm{e}^{-2\mathrm{i}\omega\tau/\varepsilon} & 0\end{bmatrix}\begin{bmatrix}A\\B\end{bmatrix}$$

with

$$m=(\eta+\nu)/2$$
$$n=(\eta-\nu)/2.$$

This gives a Ricatti equation for the reflection coefficient:

$$\frac{\mathrm{d}R}{\mathrm{d}x}=\frac{-\mathrm{i}\omega}{\sqrt{\varepsilon}}\left(\frac{\rho_0}{K_0}\right)^{1/2}[n\mathrm{e}^{2\mathrm{i}\omega\tau/\varepsilon}+2mR+nR^2\mathrm{e}^{-2\mathrm{i}\omega\tau/\varepsilon}]+\frac{1}{4}\frac{(\rho_0K_0)'}{(\rho_0K_0)}[\mathrm{e}^{2\mathrm{i}\omega\tau/\varepsilon}-R^2\mathrm{e}^{-2\mathrm{i}\omega\tau/\varepsilon}].\tag{24}$$

It remains to choose boundary conditions for R. For a statistically homogeneous medium the wave cannot penetrate to infinite depth and as in [5] we choose a 'totally reflecting termination' when analysing (24). That is, we write

$$R(x,\omega)=\mathrm{e}^{-\mathrm{i}\psi(x,\omega)}$$

with ψ real. This can be justified by embedding a finite section of the medium in a large statistically homogeneous section where the wave localizes, so that asymptotically R has unit

modulus, and finally truncate by a homogeneous section where a physical boundary condition for R can be imposed. This we can do without changing the solution due to hyperbolicity of the original problem. The method of functionals referred to above does not require such assumptions about the whole medium as it works in the time domain.

Let $\psi_{1,2}(x,\omega) = \psi(x, \omega \mp \varepsilon h/2)$, then

$$\hat{\mathcal{R}} = \mathbb{E}[\mathrm{e}^{\mathrm{i}(\psi_2(0,\omega)-\psi_1(0,\omega))}]. \tag{25}$$

We shall approximate this expectation by integrating with respect to the distribution of $\psi_2 - \psi_1$ in the small ε limit corresponding to scattering associated with the random medium taking place on a very fine scale.

For $\Psi = [\psi_1, \psi_2]$ we can write

$$\frac{\mathrm{d}\Psi}{\mathrm{d}x} = \varepsilon^{-1} F(\Psi) + G(\Psi), \tag{26}$$

with $F = [F_1, F_2]$, $G = [G_1, G_2]$ and

$$F_1 = \frac{2\omega}{\sqrt{\varepsilon}}\sqrt{\frac{\rho_0}{K_0}}[m + n\cos(\psi_1 + 2\omega\tau/\varepsilon - h\tau)]$$

$$G_1 = -\frac{1}{2}\frac{(\rho_0 K_0)'}{\rho_0 K_0}\sin(\psi_1 + 2\omega\tau/\varepsilon - h\tau) - \sqrt{\varepsilon}h\sqrt{\frac{\rho_0}{K_0}}[m + n\cos(\psi_1 + 2\omega\tau/\varepsilon - h\tau)]$$

and F_2, G_2 defined similarly. Note that m, n have zero mean and thus F is centred with respect to their distribution. The asymptotic theory for systems of the form (26) is well known, see for instance [1,5,11]. In [1,11] the case with a constant background medium was considered. Using the perturbation of generator approach as in [5] we can generalize this to the above case. The result is that if we make the change of variables

$$\psi = \psi_2 - \psi_1$$
$$\tilde{\psi} = 1/2(\psi_2 + \psi_1),$$

then we find that the associated infinitesimal generator in the small ε limit is

$$\mathcal{L}_x(\omega) = \frac{4\omega^2}{c_0^2(x)}\left\{\alpha_{s,n}(2c_0(x)\omega)/2\frac{\partial}{\partial\tilde{\psi}} + \alpha_{c,n}(2c_0(x)\omega)\left[\frac{1}{4}\frac{\partial^2}{\partial\tilde{\psi}^2} + \frac{\partial^2}{\partial\psi^2} + \cos(\psi + 2hx)\left(\frac{1}{4}\frac{\partial^2}{\partial\tilde{\psi}^2} - \frac{\partial^2}{\partial\psi^2}\right)\right] + \alpha\frac{\partial^2}{\partial\tilde{\psi}^2}\right\} \tag{27}$$

with

$$\alpha = \int_0^\infty \mathbb{E}[m(0)m(s)]\,\mathrm{d}s$$

$$\alpha_{c,n}(\omega) = \int_0^\infty \mathbb{E}[n(0)n(s)]\cos(\omega)\,\mathrm{d}s$$

$$\alpha_{s,n}(\omega) = \int_0^\infty \mathbb{E}[n(0)n(s)]\sin(\omega)\,\mathrm{d}s.$$

The coefficients in (27) do not depend on $\tilde{\psi}$ and hence ψ is Markovian by itself. We now specialize to the case with uniform background and $c(x) \equiv 1$. Then we can solve the backward Kolmogorov equation associated with (27) explicitly:

$$\frac{\partial V}{\partial x} - 4\omega^2\alpha_{c,n}(2\omega)(1 - \cos(\psi + 2hx))\frac{\partial^2}{\partial\psi^2}V = 0.$$

In view of 25 we find that

$$\hat{\mathcal{R}} = \lim_{x\to\infty} V(x,\psi),$$

when

$$V|_{x=0} = \mathrm{e}^{\mathrm{i}\psi}.$$

The limit does not depend on ψ and using (23) we get the desired result (14). The general case with $c_0 = c_0(x)$ leads to an infinite-dimensional system of equations similar to the system derived in [5].

6.4. Stabilization

The stabilization of the refocused pulse follows as in [4, 14] if we can show that the quadratic Green's operator R decorrelates for different frequencies:

$$\begin{aligned}\hat{\mathcal{R}}(\omega_a,\omega_b) &= \mathbb{E}[\mathrm{e}^{\mathrm{i}(\psi_2(0,\omega_a)-\psi_1(0,\omega_a))}\mathrm{e}^{\mathrm{i}(\psi_2(0,\omega_b)-\psi_1(0,\omega_b))}]\\ &\sim \mathbb{E}[\mathrm{e}^{\mathrm{i}(\psi_2(0,\omega_a)-\psi_1(0,\omega_a))}]\mathbb{E}[\mathrm{e}^{\mathrm{i}(\psi_2(0,\omega_b)-\psi_1(0,\omega_b))}] \qquad \text{as } \varepsilon\downarrow 0. \end{aligned} \tag{28}$$

This decorrelation entails that the second centred moment of the refocused pulse is small in the small ε limit. If we define $\Psi_2(\omega_a,\omega_b) = [\psi(\omega_a), \tilde{\psi}(\omega_a)\psi(\omega_b), \tilde{\psi}(\omega_b)]$, then the associated infinitesimal generator becomes

$$\mathcal{L}_x(\omega_a,\omega_b) = \mathcal{L}_x(\omega_a) + \mathcal{L}_x(\omega_b) - \omega_a\omega_b\alpha\frac{\partial}{\partial\tilde{\psi}_a}\frac{\partial}{\partial\tilde{\psi}_b}.$$

Since the infinitesimal generator associated with Ψ_2 is the sum of the ones associated with the single-frequency cases up to a differential term in $\tilde{\psi}_a$ and $\tilde{\psi}_b$ we find that (28) is satisfied and that the fluctuations in the refocused pulse are relatively small.

7. Conclusions

We have analysed refocusing of time-reversed wave reflections. In this problem the presence of several scales is important, as well as how these separate. We gave a simple interpretation of how stable refocusing can be interpreted in terms of averaging and illustrated it with numerical simulations. We analysed in detail acoustic waves and characterized precisely the refocusing in this case using limit theorems for stochastic ordinary differential equations.

Acknowledgments

This work was supported by NSF grant DMS-0093992 and ONR grant N00014-02-1-0090.

References

[1] Ash M, Kohler W, Papanicolaou G C, Postel M and White B 1991 Frequency content of randomly scattered signals *SIAM Rev.* **33** 519–625

[2] Bailly F and Fouque J P in progress

[3] Berryman J, Borcea L, Papanicolaou G and Tsogka C 2002 Statistically stable ultrasonic imaging in random media *J. Acoust. Soc. Am.* submitted

[4] Blomgren P, Papanicolaou G and Zhao H 2002 Super-resolution in time-reversal acoustics *J. Acoust. Soc. Am.* **111** 230–48

[5] Burridge R, Papanicolaou G, Sheng P and White B 1989 Probing a random medium with a pulse *SIAM J. Appl. Math.* **49** 582–607

[6] Clouet J F and Fouque J P 1997 A time-reversal method for an acoustical pulse propagating in randomly layered media *Wave Motion* **25** 361–8
[7] Dowling D R and Jackson D R 1992 Narrow-band performance of phase-conjugate arrays in dynamic random media *J. Acoust. Soc. Am.* **91** 3257–77
[8] Fink M 1999 Time-reversed acoustics *Sci. Am.* **November** 91–7
[9] Fink M 1993 Time reversal mirrors *J. Phys. D: Appl. Phys.* **26** 1333–50
[10] Kuperman W A, Hodgkiss W S, Song H C, Akal T, Ferla C and Jackson D R 1997 Phase conjugation in the ocean: experimental demonstration of an acoustic time-reversal mirror *J. Acoust. Soc. Am.* **103** 25–40
[11] Lewicki P and Papanicolaou G 1994 Reflection of wavefronts by randomly layered media *Wave Motion* **20** 245–60
[12] Papanicolaou G and Weinryb S 1994 A functional limit theorem for waves reflected by a random medium *Appl. Math. Opt.* **30** 307–34
[13] Thomas J L and Fink M 1996 Ultrasonic beam focusing through tissue inhomogeneities with a time reversal mirror: Application to transskull therapy *IEEE Trans. Ultrason. Ferroelectr. Freq. Control* **43** 1122–9
[14] Ryzhik L, Papanicolaou G C and Sølna K The parabolic approximation and time reversal in a random medium unpublished
[15] Sølna K 2001 Estimation of pulse shaping for well logs *Geophysics* **66** 1605–11
[16] Sølna K and Papanicolaou G 2000 Ray theory for a locally layered medium *Waves Random Media* **1** 151–198